Arch. Metall. Mater. **69** (2024), 2, 761-773

DOI: https://doi.org/10.24425/amm.2024.149808

K. KRYSTEK[1,2], I. DUL[2], M. WIERZBIŃSKA[1], M. MOTYKA[1*]

EFFECT OF VACUUM BRAZING CONDITIONS OF INCONEL 718 SUPERALLOY SHEETS ON MICROSTRUCTURE AND MECHANICAL PROPERTIES OF JOINTS

Vacuum furnace brazing is one of the most commonly used joining processes in the aerospace industry, utilized in the manufacturing of the complex components of turbine jet engines, working in both their cold and hot sections. The modern aerospace industry demands continuous improvement of production processes to enhance the engine performance, while ensuring its reliability. Therefore, a better understanding of the processes that shape the properties of engine assemblies joints is crucial. This paper presents an analysis of the influence of key brazing process parameters – brazing time and gap width – on the microstructure and mechanical properties of Inconel 718 superalloy joints obtained with the Palnicro 36M filler alloy. The analysis was conducted basing on results from SEM/EDS analysis and peel, shear and spreadability tests.

Keywords: Ni-based superalloy; vacuum brazing; brazing filler metal; microstructure; SEM/EDS analysis

1. Introduction

Inconel 718 is one of the most widely used nickel superalloys in the industry, accounting for more than 50% of the total superalloy market [1]. Despite its development in late 1950s [2], it is still extensively used in aerospace and energy applications to this day. Alloy 718 popularity results from its properties – excellent corrosion resistance and very good mechanical characteristics, which can be maintained up to 650°C, connected with good processability [1,3]. In modern gas turbine engines for aviation industry, it is used for both rotating elements, like shafts, disks and blades, and stator assemblies like casings and exhaust ducts [4]. In accordance with Pratt & Whitney's data, alloy 718 constituted 57% of the total weight of nickel superalloys used for PW4000 engine construction [5]. Inconel 718 is a precipitation hardenable alloy. Its main strengthening phase is metastable, body-centered tetragonal γ" phase (Ni_3Nb). After prolonged exposure to temperature above 650°C, γ" precipitates dissolves and transforms into thermodynamically stable, orthorhombic δ-Ni_3Nb phase, resulting in decrease of the alloy mechanical properties [6-9]. Therefore, proper heat treatment of elements made of alloy 718 is crucial in terms of their performance. Optimal heat treatment, offering good mechanical characteristics and highest fatigue strength, consists of two operations: solutionizing from the temperature withing range of 927-1010°C, followed by two-step precipitation hardening – first in 718°C for 8 hours and then in 621°C for a total time of 18 hours [9].

In construction of complex assemblies used in modern aircraft engines, choosing a proper method of joining is a crucial part of the process. Brazing with nickel-based filler metal alloys is a well-known and commonly used method of joining the components made of superalloys for turbine engine applications, offering good mechanical properties of the joints and excellent corrosion resistance [10,11]. However, due to high melting point of nickel, alloys from this group require usage of so-called melting point depressants (MPD), usually boron, silicon or phosphorus, which presence may lead to the formation of very hard, brittle phases [11,12].

In industrial practice, brazing of elements made of Inconel 718 is typically done concurrently in one operation with solutionizing. Incorrect heat treatment may lead to undesirable microstructural changes, detrimental for the alloy mechanical properties [13-14]. Moreover, its chemical composition consists of chromium, aluminum and titanium additions, creating very stable, hard to dissociate oxides, significantly decreasing wettability of the surface [15]. That is why alloy 718 is considered a difficult-to-braze material and better understanding of factors influencing evolution of the joint microstructure in different

[1] RZESZOW UNIVERSITY OF TECHNOLOGY, DEPARTMENT OF MATERIALS SCIENCE, 12. POWSTAŃCÓW WARSZAWY AV., 35-959 RZESZÓW, POLAND
[2] PRATT & WHITNEY RZESZÓW S.A., 120 HETMAŃSKA STR., 35-078 RZESZÓW, POLAND

* Corresponding author: motyka@prz.edu.pl

processing conditions is an important research issue, which should be continuously investigated. Linkiewicz et al. [16] investigated the impact of alloy 718 surface preparation on wettability with BNi-3 alloy, showing that nickel plating is offering the best results in that matter. Many researchers focus on the relation of the processing parameters with microstructure evolution and mechanical properties of the joints. Puranvari et al. analyzed impact of the filler metal chemical composition on precipitation processes in joints of Inconel 718 brazed with BNi-2, BNi-3 and BNi-9 alloys [17] and impact of the full heat treatment cycle on properties of cast 718/BNi-2 joints [18]. Yan et al. studied the impact of brazing temperature [19] and post-brazing treatment on properties of the joints from wide gap brazing process on alloy 718 [20]. Another area of researchers interest is investigation of joints with different materials, such as ultrafine grained AISI 304L steel [21], Waspaloy [22] or Inconel 625 [23].

The main issue with usage of the filler metals from the BNi group for Inconel 718 brazing is their liquidus temperature above 1000°C, which is related with significant risk of base metal grain coarsening [24]. A solution to that problem may be nickel-based palladium-rich filler metals (e.g. Palnicro® alloys), offering excellent work characteristics at elevated temperatures and melting point below 1000°C. Despite of fact that brazing of Inconel 718 with such alloys was investigated in recent decades [15,24-25], available information regarding this process is still limited. Therefore, the aim of this paper is the investigation of the impact of brazing time and gap on properties of the Inconel 718/Palnicro 36M joints in process of brazing concurrent with solution heat treatment and after precipitation hardening.

2. Materials and experiment

Precipitation hardenable, nickel-based superalloy Inconel 718 in the form AMS5596 sheet was used in present experiment as the base metal (BM). It was brazed with Palnicro 36M (Ni-36Pd-10,5Cr-3B-0,5Si) brazing filler metal (BFM) in the form of paste and – in the case of spreadability tests – 0,05 mm foil, manufactured by Morgan Advanced Materials (TABLE 1). The liquidus temperature of this alloy is 960°C and its recommended brazing temperature range is 970-1050°C. As it offers excellent creep resistance and can be melted below 1000°C, it is commonly used for joining assemblies made of Inconel 718 for turbine engine applications, working at elevated temperature [26].

Standardized set of specimens with a width of 2.54 mm was adopted in the experiment, dedicated for: metallographic examination – flat specimens brazed in a lap configuration (Fig. 1a), shear test – flat specimens brazed in a lap configuration (Fig. 1b), peel test – L-shaped specimens brazed in a double-L (referred also as T) configuration mm (Fig. 1c), spreadability test – single sheet specimens with filler in form of foil discs (Fig. 1d).

The experiment consisted of two stages, aimed for investigation of different processing factors impact on microstructure and mechanical properties of the joint. In the first stage, effect of the time at brazing temperature was investigated. Brazing was carried out concurrently with solution heat treatment. In case of such processes, the assembly is heated to brazing temperature, held in that temperature for the brazing time, and then temperature is lowered to the BM solutionizing temperature, then soaked for the time remaining to reach required solutionizing time. In accordance with Inconel 718 manufacturers data, optimal solutionizing time and temperature for this alloy is 60 min and 954°C, respectively [9], so these parameters were used. Therefore, "brazing time" should be understood as a portion of the hold time in brazing temperature and taken for test was t_b = 1, 3, 10, 20, 30, 45 and 60 min for nominal brazing gap g_b = 0.05 mm (Tab. 2). Samples for the metallographic (Fig. 1a), shear (Fig. 1b), peel (Fig. 1c) and spreadability (Fig. 1d) test were used in this test segment.

The second part of the study was dedicated to the impact of the brazing gap width on joint properties. Process parameters were constant (brazing time 10 min, solutionizing time 50 min), and the variable was brazing clearance. Values taken for the analysis were g_b = 0.05, 0.1, 0.15, 0.2, 0.3, 0.4 and 0.5 mm. Samples

TABLE 1

Chemical composition of investigated alloys [9,26]

Alloy	Element, % wt.											
	Ni	Cr	Fe	Mo	Co	C	Nb	Ti	Al	Si	B	Pd
Inconel 718	bal.	19	18	3	≤1	≤0.08	5.1	0.9	0.5	—	—	—
Palnicro 36M	bal.	10.5	—	—	—	—	—	—	—	0.5	3	36

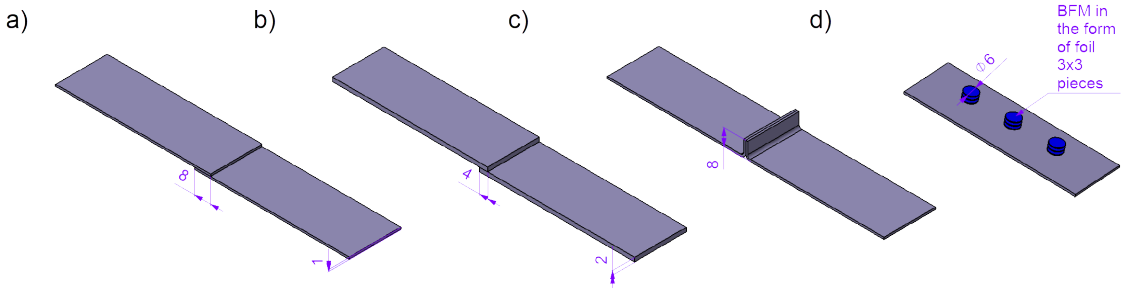

Fig. 1. Samples used for a) metallographic, b) shear, c) peel d) spreadability test. Dimensions given in mm

for metallographic (Fig. 1a), shear (Fig. 1b) and peel (Fig. 1c) test were used. In both segments, samples for metallographic and shear tests were doubled and the second set of samples was subjected to the precipitation hardening, to evaluate processing parameters impact on the joint in aged condition. Each joint has been given individual marking to facilitate identification. Parameters used in each study segment and joint designation were summarized in TABLE 2.

For each particular test, surface of samples was prepared by nickel plating process. Coating thickness was selected in accordance with AMS recommendations and was within the range of 0.005-0.015 mm [27]. Samples were assembled using ball-tack welding method with 1 mm stainless steel balls. The clearance was set using a feeler gauge. BFM was applied at one edge of the joint, except for spreadability test samples, where BFM in form of prefabricated, 6 mm foil discs was used (Fig. 1d). Process was carried out in industrial conditions, in Seco/Warwick VP-4050/72HV vacuum (0.1 Pa or lower) furnace.

Metallographic specimens were prepared using standard laboratory methods. If required for better microstructure picturing, it was etched with solution of 15 ml HNO_3, 15 ml CH_3COOH, 60 ml HCl and 15 ml distilled water. Microstructure and chemical composition in selected areas of joints was investigated with Scanning Electron Microscopy (SEM) using Hitachi S-3400N microscope equipped with Thermo energy dispersive X-ray spectroscopy (EDS) detector.

The shear test was done using Zwick/Roell Z100 universal tensile machine. Thickness of BM and overlap length was selected in a ratio ensuring the localization of the fracture in the joint. Maximum braking force was determined in the test. Basing on that and measured dimensions of the joint, shear strength was calculated in accordance with (2.1):

$$R_t = \frac{F_{\max}}{A \cdot W} \tag{2.1}$$

Where R_t is the shear strength, $F_{\max}$ is the maximum breaking force, A is overlap length and W is joint width. In spreadability test, surface area of the melted BFM was measured using stereoscopic microscope. Final surface area of the spread filler alloy for particular test was calculated as a arithmetic mean from surface area of three portion of the BFM, where areas of each of these portions were calculated basing on arithmetic mean of two perpendicular diameters (Fig. 2), in accordance with (2.2) and (2.3):

$$\overline{d} = \frac{\frac{d_1 + d_2}{2} + \frac{d_3 + d_4}{2} + \frac{d_5 + d_6}{2}}{3} \tag{2.2}$$

$$\overline{P_p} = \pi \left(\frac{\overline{d}}{2} \right)^2 \tag{2.3}$$

Where $\overline{P_p}$ is average surface area of spread filler alloy.

TABLE 2

Process parameters of brazed specimens

Brazing time in 996°C t_b , min	Brazing gap g_b, mm	Solutionising parameters	Specimen designations	Ageing parameters	Specimen designations
1	0.05	954°C for, 60 min – t_b, rapid cooling	T1/S	732°C for 8h, cooling with furnace to 621°C, holding in 621°C for 8 h, rapid cooling	T1/S/A
3	0.05		T3/S		T3/S/A
10	0.05		T10/S		T10/S/A
20	0.05		T20/S		T20/S/A
30	0.05		T30/S		T30/S/A
45	0.05		T45/S		T45/S/A
60	0.05		T60/S		T60/S/A
10	0.05		G5/S		G5/S/A
10	0.1		G10/S		G10/S/A
10	0.15		G15/S		G15/S/A
10	0.20		G20/S		G20/S/A
10	0.3		G30/S		G30/S/A
10	0.4		G40/S		G40/S/A
10	0.5		G50/S		G50/S/A

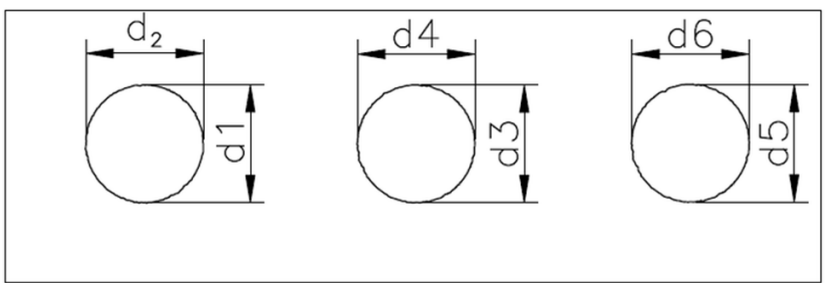

Fig. 2. Methodology of diameter measurement in spreadability test used in the study

Peel test was done using Zwick/Roell Z100 universal tensile machine. Evaluation of the fracture surface was carried out using a stereoscopic microscope to determine the coverage given in %, with an accuracy of 5%. If the fracture was partially or completely localized in the BM, these parts of the joint were separated using manual methods. Subsequently, undamaged areas were evaluated, and in the damaged areas the coverage was assumed to be 100%.

3. Results

3.1. Impact of brazing time on joints' properties

3.1.1. Microstructure

In joint brazed for 1 minute, significant unevenness of the brazing gap was found, resulting from non-parallel positioning of joined sheets. In this case, analysis was done in the area where gap width was approximately 100 µm. No lack of parallelism was noticed in other joints, where obtained gap width was in range of 40-80 µm. Observed microstructure is typical for joints brazed with nickel-based filler alloys containing MPD, where several characteristic zones can be distinguished. BM microstructure unaffected by the diffusion is composed of γ-Ni phase, without clearly visible grain boundaries and with occasional Nb-rich phases (Fig. 3a). Closer to the joint, diffusion zone (DZ) can be observed. In the case of filler alloys containing boron and silicon MPD, this zone is formed predominantly due to the diffusion of boron atoms into the BM matrix [28-29]. Morphology of DZ is similar in each joint, regardless of the brazing time – it is formed by very fine, globular precipitates. Leading role of boron in diffusional evolution of DZ and chemical composition analysis of this zones (Fig. 3a, area 2, TABLE 3), revealing significantly increased amount of this element, confirms that borides are its main phase constituent.

The most differences in microstructure can be observed in the braze zone in centre of the joint. In the joint brazed for 1 (Fig. 3a) and 3 (Fig. 4a) min, significant heterogeneity of the microstructure was observed in this area. In the centerline of the braze formed so-called athermal solidification zone (ASZ). It is a characteristic, multi-phase zone formed during the cooling from the remaining, liquid portion of the filler metal that was unable to solidify isothermally during brazing. Due to high

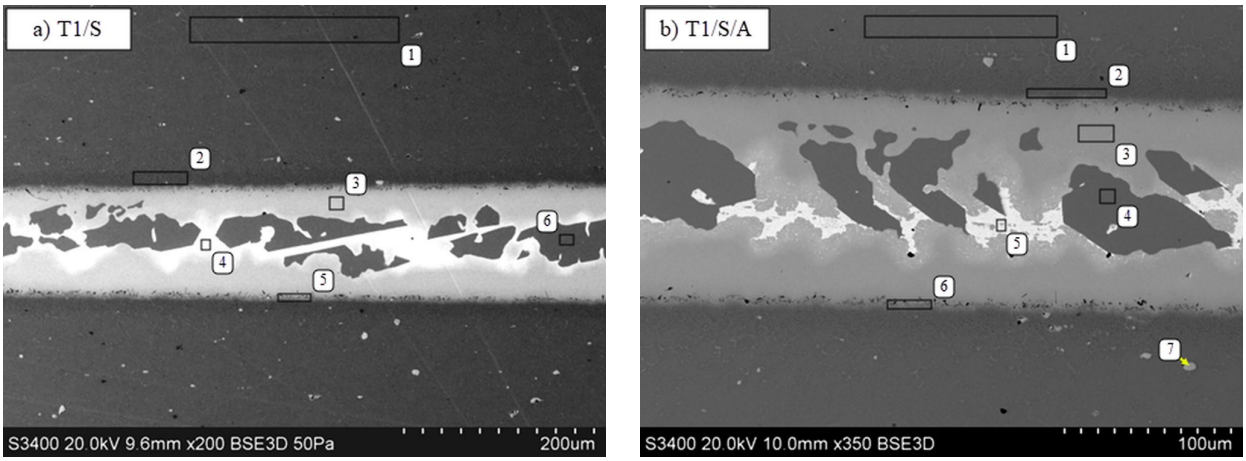

Fig. 3. Microstructure of Inconel 718/Palnicro 36M joints brazed for 1 minute with solutionizing (a) and after precipitation hardening (b)

TABLE 3

Chemical composition in selected areas of T1/S (Fig. 3a) and T1/S/A (Fig. 3b) joints

Joint	Area	Element, % at.								
		B-K	Si-K	Ti-K	Cr-K	Fe-K	Ni-K	Nb-L	Mo-L	Pd-L
T1/S	1	—	—	1.3	21.0	20.0	52.7	3.2	1.8	—
	2	10.4	0.4	1.3	21.3	18.7	40.9	3.7	1.9	1.4
	3	4.0	1.1	—	15.6	4.6	55.0	—	—	19.7
	4	13.2	20.8	—	—	—	14.2	—	—	51.8
	5	3.8	—	—	17.2	12.4	54.4	1.9	1.6	8.7
	6	—	—	—	6.4	2.7	85.9	—	—	5.0
T1/S/A	1	—	—	1.3	21.1	20.3	52.1	3.5	1.7	—
	2	12.1	—	1.2	22.1	19.7	38.9	3.9	2.1	—
	3	—	1.3	—	15.8	—	58.7	—	—	24.2
	4	—	—	—	3.5	—	91.9	—	—	4.6
	5	10.1	21.0	—	—	—	9.5	—	—	59.4
	6	4.0	—	—	20.7	13.0	51.9	2.5	2.0	5.9
	7	14.5	—	16.1	—	—	—	68.2	1.2	—

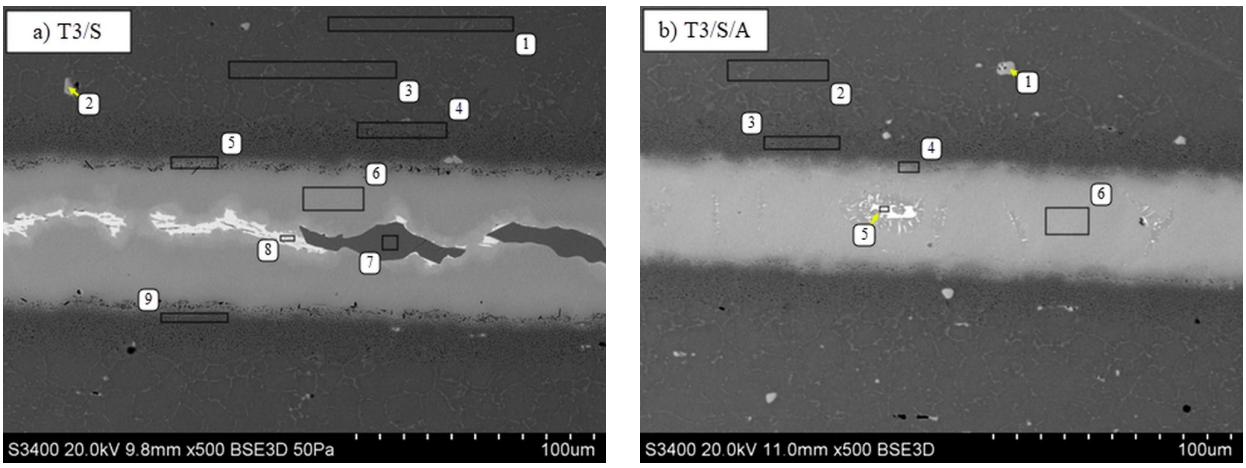

Fig. 4. Microstructure of Inconel 718/Palnicro 36M joints brazed for 3 minute with solutionizing (a) and after precipitation hardening (b)

TABLE 4

Chemical composition in selected areas of T3/S (Fig. 4a) and T3/S/A (Fig. 4b) joints

Joint	Area	Element, % at.								
		B-K	Si-K	Ti-K	Cr-K	Fe-K	Ni-K	Nb-L	Mo-L	Pd-L
T3/S	5	4.3	0.6	0.8	21.0	13.8	48.9	2.6	2.2	5.8
	6	—	1.4	—	15.4	5.2	59.0	—	—	19.0
	7	—	—	—	7.3	3.4	84.5	—	—	4.9
	8	14.1	16.1	—	7.2	4.3	25.7	—	—	32.6
T3/S/A	9	10.8	0.4	—	21.5	15.9	42.7	3.4	2.1	3.2
	4	—	0.7	—	17.8	10.8	58.9	1.3	1.9	8.7
	5	9.7	16.4	—	4.1	—	23.3	—	—	46.5
	6	—	2.0	—	13.4	1.9	60.1	—	—	22.6

concentration of MPD, it consists of hard and brittle compounds, therefore formation of this zone is considered detrimental for the joint properties and should be prevented. In the case of Inconel 718/Palnicro 36M joint brazed for 1 minute ASZ consist of two phase components. First, visible in the microstructure as a dark-grey, plate-like areas, is Ni-Pd-Cr-Fe (85.9/5/6.4/2.7% at. – Fig. 3a, area 6, TABLE 3) phase. The second one is Pd-Ni-Si-B (65/14.2/20.8/13.2% at. – Fig. 3a, area 4, TABLE 3), creating continuous, white bands, filling the space between Ni-Pd-Cr-Fe precipitates. The rest of the braze zone is single-phase, austenitic γ-Ni solid solution, crystalized during brazing and located near the braze-BM phase boundary, forming so-called isothermal solidification zone (ISZ). Similar phase composition and morphology of the braze zone was observed in T3/S joint. However, in this case, due to the significantly smaller gab, width of ASZ was notably lower. Chemical composition of particular constituents was comparable to T1/S joint – 84.5/4.9/7.3/3.4% at. for Ni-Pd-Cr-Fe phase (Fig. 4a, area 7, TABLE 4) and 32.6/25.7/16.1/14.1% at. for Pd-Ni-Si-B phase. In second phase also presence of chromium (7.2% at.) and iron (4.3% at.) was

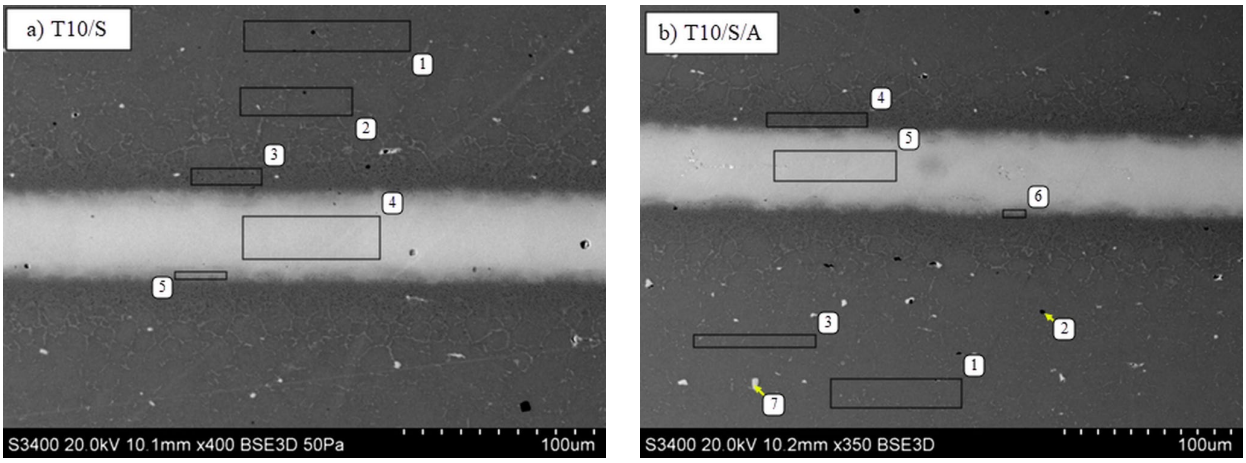

Fig. 5. Microstructure of Inconel 718/Palnicro 36M joints brazed for 10 minute with solutionizing (a) and after precipitation hardening (b)

TABLE 5

Chemical composition in selected areas of T10/S (Fig. 5a) and T10/S/A (Fig. 5b) joints

Joint	Area	Element, % at.								
		B-K	Si-K	Ti-K	Cr-K	Fe-K	Ni-K	Nb-L	Mo-L	Pd-L
T10/S	3	14.1	0.3	1.1	21.2	18.5	38.9	3.4	1.9	0.6
	4	3.9	1.2	—	16.5	5.7	56.2	—	—	16.5
	5	4.40	0.8	—	17.0	12.7	62.1	1.6	1.4	—
T10/S/A	2	—	—	87.6	—	—	—	12.4	—	—
	4	14.3	—	1.2	22.0	19.2	37.5	3.7	2.1	—
	5	—	1.5	—	14.4	1.5	60.8	—	—	21.7
	6	—	0.4	—	20.0	11.9	56.5	2.0	1.9	7.3
	7	16.1	—	12.4	4.2	—	8.1	59.1	—	—

noticed. In both joints, in braze zone directly near the BM, clusters of fine, Cr-rich precipitates (Fig. 3a, area 5, TABLE 3 and Fig. 4a, area 5, TABLE 4) were noticed.

Microstructure of the joints brazed for 10, 20 and 30 min was uniform, entirely composed of single-phase γ-Ni solid solution (Fig. 5a). Chemical composition of braze zone (TABLE 6) is representative for all joints brazed in time of 10-30 min. Presence of ASZ was noticed again in the joints with the longest analysed brazing time – 45 and 60 min. Phase composition was the same as observed in case of previous joints, however average size of Ni-Pd-Cr precipitates was significantly lower and they were more dispersed (Figs. 6a, 7a). Similarly, the amount of observable Pd-rich phase was notably decreased in comparison to joints with shorter brazing time.

Results of the microstructure analysis after precipitation hardening show considerable improvement in terms of braze zone homogeneity. In joint after brazing per 1 minute, it is observable mostly in reduction of the Pd-Ni-Si-B phase volume in ASZ (Fig. 3b). Significantly more advanced homogenisation of braze microstructure, most probably due to the smaller width of

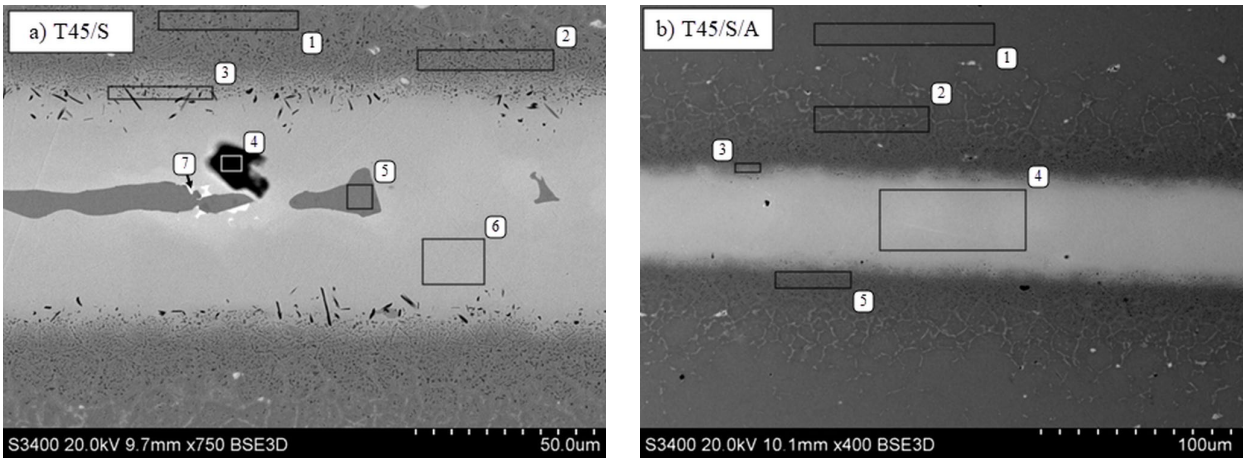

Fig. 6. Microstructure of Inconel 718/Palnicro 36M joints brazed for 45 minute with solutionizing (a) and after precipitation hardening (b)

TABLE 6

Chemical composition in selected areas of T45/S (Fig. 6a) and T45/S/A (Fig. 6b) joints

Joint	Area	Element, % at.								
		B-K	Si-K	Ti-K	Cr-K	Fe-K	Ni-K	Nb-L	Mo-L	Pd-L
T45/S	1	—	—	1.3	22.1	19.1	50.8	4.3	2.4	—
	2	11.0	—	1.2	22.7	18.4	40.4	4.0	2.3	—
	3	6.5	—	—	20.7	11.4	49.2	1.8	2.1	8.3
	4	24.1	8.3	3.7	13.5	—	26.3	—	1.1	22.9
	5	—	—	—	4.1	—	91.7	—	—	4.2
	6	4.1	1.2	—	16.4	1.6	56.2	—	—	20.5
	7	—	3.6	—	4.8	—	73.0	—	—	18.6
T45/S/A	1	—	—	—	21.6	19.7	53.3	3.3	2.0	—
	2	8.8	—	1.4	21.5	19.7	51.7	3.7	2.1	—
	3	—	0.5	—	20.1	12.0	55.8	2.0	1.9	7.6
	4	5.2	1.4	—	15.6	1.9	60.5	—	—	20.6
	5	14.1	0.4	—	22.1	19.2	52.3	3.8	2.2	—

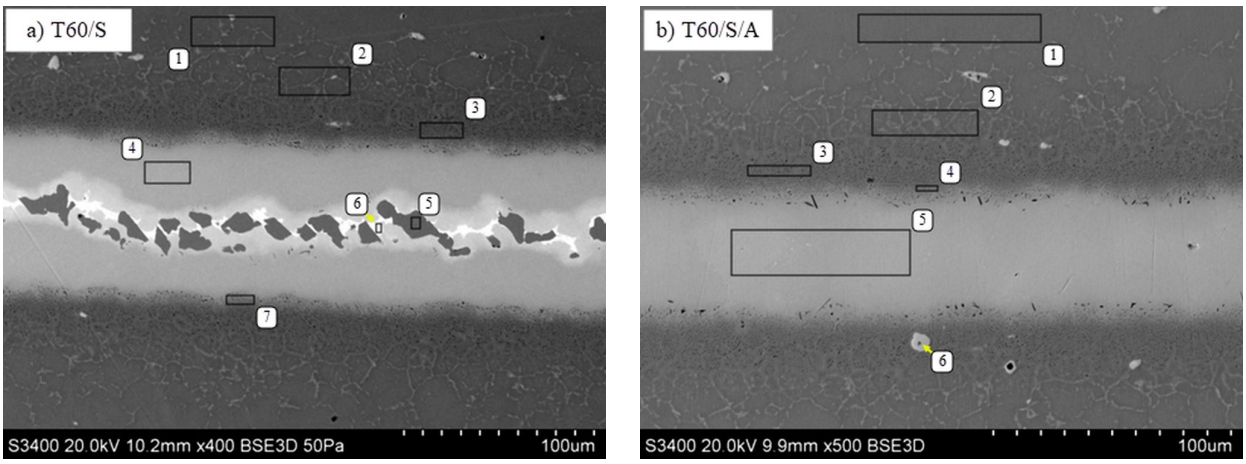

Fig. 7. Microstructure of Inconel 718/Palnicro 36M joints brazed for 60 minute with solutionizing (a) and after precipitation hardening (b)

TABLE 7

Chemical composition in selected areas of T60/S (Fig. 7a) and T60/S/A (Fig. 7b) joints

Joint	Area	Element, % at.								
		B-K	Si-K	Ti-K	Cr-K	Fe-K	Ni-K	Nb-L	Mo-L	Pd-L
	1	—	—	1.3	21.1	19.1	53.3	3.3	1.9	—
	2	6.1	0.4	1.3	20.8	18.8	46.7	3.3	1.9	0.7
	3	11.4	0.3	1.2	21.9	17.9	40.0	3.9	2.3	1.2
	4	—	1.0	—	17.2	4.8	58.5	—	—	18.6
	5	—	—	—	7.5	3.2	83.0	—	—	6.3
	6	14.3	15.8	—	7.8	—	28.5	—	—	33.6
	7	4.7	0.7	0.8	19.5	12.3	51.5	1.5	—	9.0
	1	—	—	1.2	21.3	19.6	52.9	3.2	1.8	—
	2	12.1	—	1.2	21.1	19.3	40.2	3.9	2.2	—
	3	11.4	—	1.2	22.3	18.9	40.0	4.0	2.2	—
	4	6.3	0.5	—	21.4	11.8	54.6	2.5	2.0	7.1
	5	—	1.6	—	14.6	1.9	61.5	—	—	20.4
	6	15.7	—	20.2	—	—	—	64.1	—	—

the gap, can be observed in joint after 3 min of brazing (Fig. 4b). In this case, braze zone microstructure is nearly uniform, composed of γ-Ni solid solution, with single Pd-rich precipitates (Fig. 4b, area 5, TABLE 5). In microstructure of the joint brazed for 10, 20 and 30 min there was no observable difference after precipitation hardening (Fig. 5b). In remaining joints, brazed for 30, 45 and 60 min, braze zone microstructure was uniform, with occasional, fine Cr-rich precipitates adjacent to the BM surface (Fig. 6b, 7b).

3.1.2. Shear test after brazing with solutionizing and after precipitation hardening

Results of performed shear tests, both after brazing with solutionizing and after precipitation hardening, indicate a clear upward trend within 1-10 min range of brazing time. Comparable distribution was observed in maximum breaking force (Fig. 8, TABLE 8), registered directly in the tests, as well as in shear strength calculated on its basis in relation to the surface area of

TABLE 8

Results of shear tests of Inconel 718/Palnicro 36M joints after brazing with solutionizing and variable brazing time

Specimen designation	F_{max}, N	Overlap length A, mm	Joint width, mm	Joint surface area, mm^2	Shear strength R_t, MPa
T1/S	21589	4.16	25.48	106.0	204
T3/S	22175	3.99	25.75	102.7	216
T10/S	26755	3.87	25.54	98.8	271
T20/S	38743	4.25	25.46	108.2	359
T30/S	28499	3.81	25.60	97.5	292
T45/S	33509	4.08	25.51	104.1	322
T60/S	28340	3.90	25.58	99.8	284

TABLE 9

Results of shear tests of Inconel 718/Palnicro 36M joints after brazing with solutionizing and variavle brazing tine and after precipitation hardening process

Specimen designation	F_{max}, N	Overlap length A, mm	Joint width, mm	Joint surface area, mm^2	Shear strength R_t, MPa
T1/S/A	26432	4.05	25.44	103.0	257
T3/S/A	31206	4.12	25.47	104.9	297
T10/S/A	34450	4.02	25.51	102.6	336
T20/S/A	28668	4.22	25.52	107.7	266
T30/S/A	34484	3.85	25.56	98.4	350
T45/S/A	34904	4.12	25.54	105.2	332
T60/S/A	36494	4.02	25.47	102.4	356

the joint (Fig. 9, TABLE 9). In almost every case, significant increase in mechanical properties was observed after precipitation hardening. The exception is joint brazed for 20 min, where after aging, drop of both parameters was noticed. Since this effect wasn't observed in any other joint, it is probably connected with individual issues of I/20/0,05/S joint (e.g. resulting from non-axial assembling, local contamination of the brazed surface, etc.).

3.1.3. Peel test and spreadability test

In peel test of Inconel 718/Palnicro 36M joints from processes with various brazing time, 100% of coverage was found in case of each joint (Fig. 10). These results show that for adopted overlap length – 8 mm – each tested brazing time is sufficient for complete coverage of joined surfaced with filler metal.

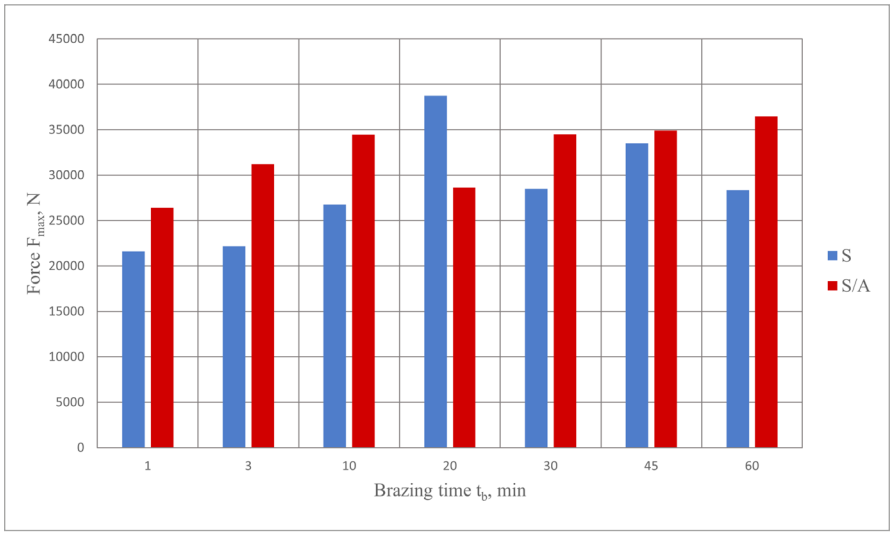

Fig. 8. Impact of the brazing time on the maximum braking force F_{max} in shear test of Inconel 718/Palnicro 36M joints

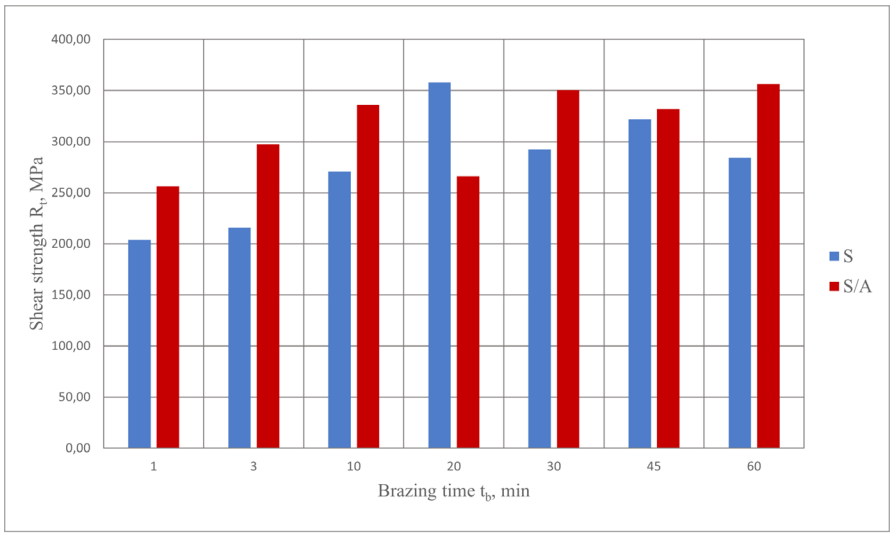

Fig. 9. Impact of the brazing time on the shear strength R_t in shear test of Inconel 718/Palnicro 36M joints

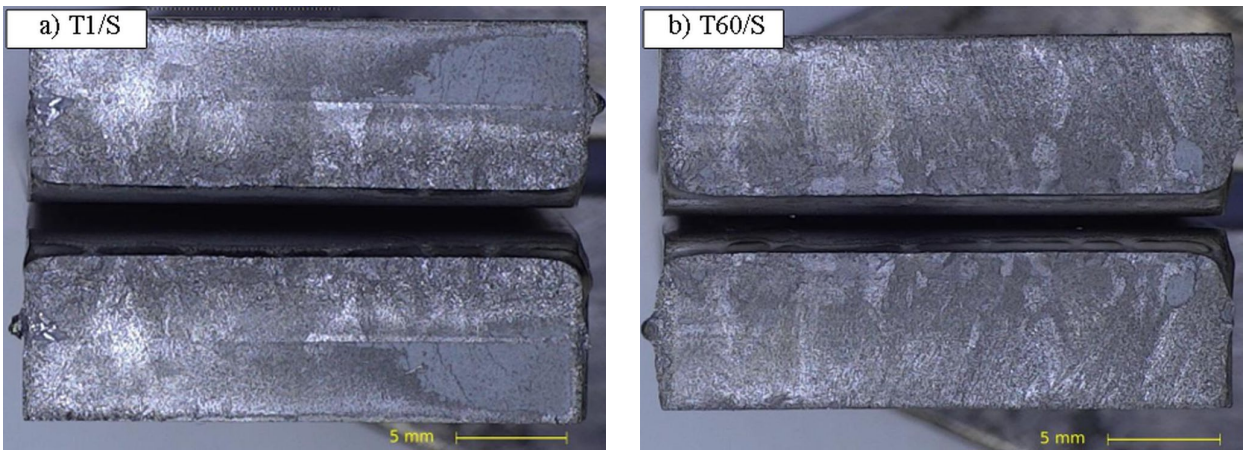

Fig. 10. View of brazed surfaces of Inconel 718/Palnicro 36M joints after peel test for brazing time of 1 (a) and 60 min (b)

The results of spreadability tests show a significant increase in filler metal flow capabilities with an increase of the brazing time within 1-20 min range (Fig. 11, TABLE 10). Average surface area of the spread BFM from the shortest analysed time (1 minute) was 45,15 mm^2, while the same parameter for 20 min of brazing time was 98,12 mm^2. Increasing of the time into the 30-60 min range did not result in further increase of the BFM spreadability. Therefore, it can be stated that in brazing of the elements made of Inconel 718 with Palnicro 36 M filler metal, there is no reason to use time longer than 20 min in terms of filler metal flow characteristics.

3.2. Impact of brazing gap on properties of the joint

3.2.1. Microstructure

In the second stage of the study, aimed for the characterization of the gap width impact, microstructure evolution was analysed through the linear distribution of elements at the joint cross-section. The joint with 0.05 mm clearance in this section is the same joint, which was presented in previous part of the research for 10 min of brazing time. As already shown, micro-

TABLE 10

Results of the spreadability test of the Palnicro 36M BFM on the Inconel 718 for brazing time in range 1-60 min (accordance with eq. 2.2, 2.3 and Fig. 2)

Joint	d_1, mm	d_2, mm	Avg.	d_3, mm	d_4, mm	Avg.	d_5, mm	d_6, mm	Avg.	$\bar{d}$, mm	$\overline{P_p}$, mm^2
T1/S/A	7.74	7.56	7.65	7.29	7.60	7.45	7.43	7.87	7.65	7.58	45.15
T3/S/A	8.58	9.15	8.86	9.02	8.80	8.91	9.28	9.42	9.35	9.04	64.19
T10/S/A	9.95	9.81	9.88	10.26	9.95	10.10	10.35	9.51	9.93	9.97	78.05
T20/S/A	10.92	10.65	10.79	11.14	10.57	10.85	11.85	11.94	11.89	11.18	98.12
T30/S/A	11.85	10.96	11.41	11.67	11.01	11.34	10.65	10.43	10.54	11.10	96.70
T45/S/A	9.77	9.90	9.84	10.70	10.21	10.46	10.04	10.57	10.30	10.20	81.67
T60/S/A	13.97	10.35	12.16	11.23	8.27	9.75	11.94	10.35	11.14	11.02	95.30

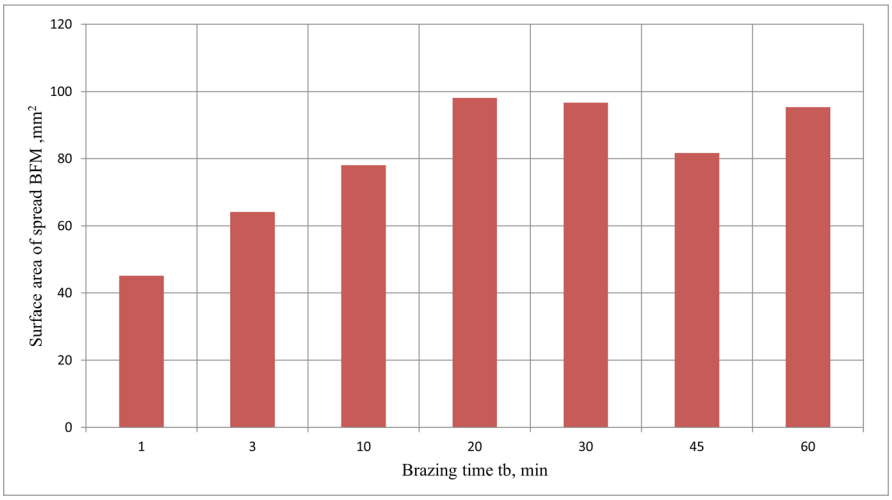

Fig. 11. Impact of the brazing time on spreadability of the Palnicro 36M BFM on the Inconel 718 superalloy

structure of this joint is uniform, composed entirely of γ-Ni solid solution. Characteristic of the elements distribution in that case is related to the differences in chemical composition of specific alloys – significant raise in palladium, along with drop with chromium content, can be observed after crossing the BM-BFM phase boundary (Fig. 12a). Increasing the brazing gap to 0.01 mm is sufficient enough for athermal crystallization phenomenon to occur. ASZ can be spotted at entire length of central area of the G10/S joint (Fig. 12c). It is composed of Ni-Pd-Cr phase and Pd-Ni-Si-B phase crystals, which morphology is analogous to this previously observed. Further increase of the brazing gap, from 0.15 mm (Fig. 12e) to 0.5 mm (Fig. 12g), resulted in a continuous and repetitive evolution of the microstructure. Similarly to previously observed joints, predominant phase component were Ni-Cr-Pd crystals, between which bands of Pd-rich precipitates were observed. Relative volume of ASZ increased along with the gap width, until it completely filled the braze zone above the 0.3 mm gap (Fig. 12i). It can be also observed that wider gap promotes greater dispersion of the precipitates. Linear distribution of elements in the joints with ASZ are typical to the multiphase microstructure, with observable, step change in amount of Cr, Pd and Ni, being a good visualisation of the differences in chemical composition between phases in the braze zone (Fig. 12). Presented study didn't show any significant impact of the gap width on diffusion zone depth or morphology.

In single-phase, 0.05 mm gap joint after precipitation hardening there was no observable changes in microstructure (Fig. 12b). In majority of the joints containing ASZ, the most noticeable effect of this operation was once again the reduction of the Pd-rich phase relative volume, which is particularly evident in joints with a gap width of 0.2 mm (Fig. 12h), 0,3 mm (Fig. 12j) and 0,4 mm (Fig. 12l). Furthermore, the microstructure of G20/S/A (Fig. 12h) and G30/S/A (Fig. 12j) joints indicates the potential occurrence of fragmentation and an increase in the degree of Ni-Pd-Cr phase dispersion. Another effect of the final heat treatment appears to be the presence of a large number of very fine, chromium-rich precipitates throughout the volume of the braze zone. In the case of widest analysed gap, larger precipitates of this phase were also observed (Fig. 12n). Despite of that, no other observable effect on the morphology of the multiphase, ASZ zone can be seen after precipitation hardening. Linear distributions of the key elements indicate a lack of significant differences in the chemical composition of the particular phase components between individual processing states (Fig. 12).

3.2.2. Shear test after brazing with solutionizing and after precipitation hardening

The results of the shear tests, in both heat treatment states, demonstrated the highest strength in joints with the smallest brazing gaps (TABLES 11 and 12, Fig. 13). Shear strength of joints after brazing with solutionizing decreases with an increase in gap width – from R_t = 271 MPa for a 0.05 mm gap to 179 MPa for a 0.5 mm gap (TABLE 11). Precipitation hardened joints exhibit higher strength values – from R_t = 336 MPa for a 0.05 mm gap, to 201 MPa for a 0.5 mm gap (TABLE 12). This trend is not unequivocal within the 0.15 to 0.4 mm gap range, necessitating more detailed tests supported by statistical analysis.

3.2.3. Peel test

In the peel test of Inconel 718/Palnicro 36M joints, within the adopted range of gap width, complete, 100% coverage of the joined surfaces was observed for the smallest values: 0.05 (Fig. 14a), 0.1 and 0.15 mm. As the gap width increased, a gradual decrease in coverage was noted, from 88% for the joint G20/S

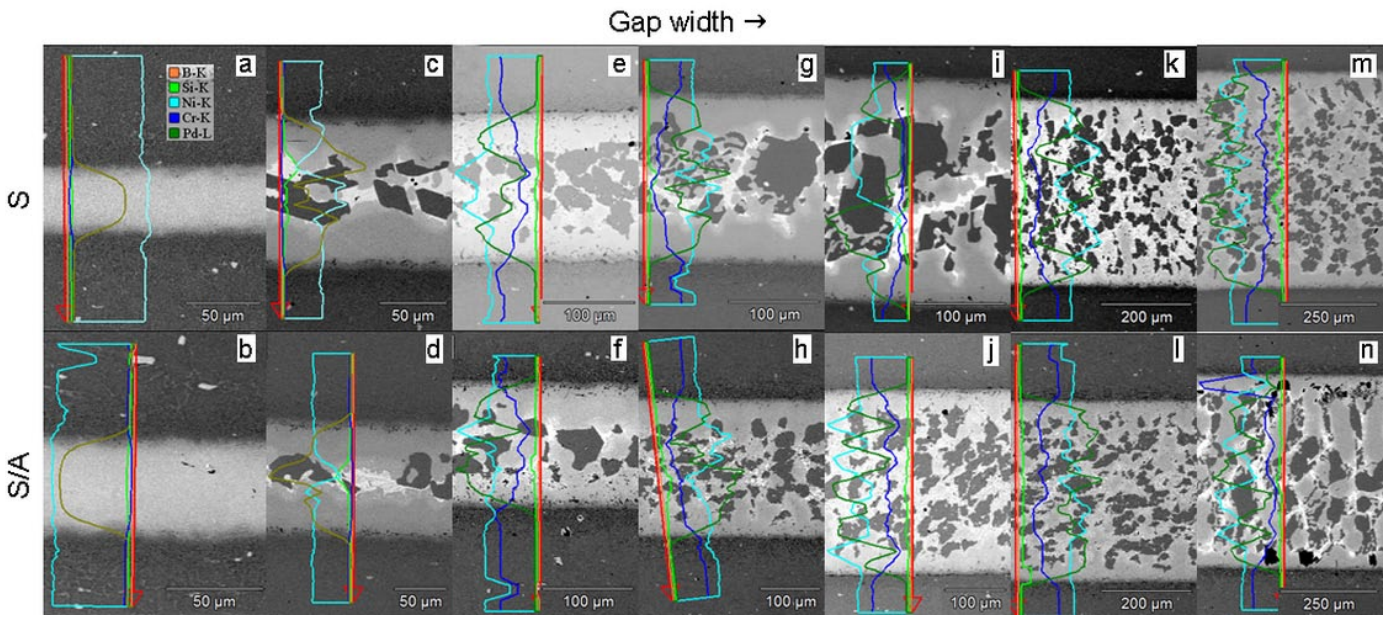

Fig. 12. Microstructure of Inconel 718/Palnicro 36M joints with various gap after brazing with solutionizing (a, c, e, g, i, k, m) and precipitation hardening (b, d, f, h, j, l, n)

TABLE 11

Results of shear tests of Inconel 718/Palnicro 36M joints with various brazing gap after brazing with solutionizing

Specimen designation	F_{max}, N	Overlap length A, mm	Joint width, mm	Joint surface area, mm^2	Shear strength R_t, MPa
G5/S	26755	3.87	25.54	98.8	271
G10/S	24152	3.98	25.50	101.5	238
G15/S	20854	4.14	25.47	105.5	198
G20/S	20732	4.15	25.49	105.8	196
G30/S	20416	4.09	25.46	104.1	196
G40/S	20366	4.17	25.47	106.2	192
G50/S	18654	4.08	25.49	104.0	179

TABLE 12

Results of shear tests of Inconel 718/Palnicro 36M joints with various brazing gap after brazing with solutionizing and after precipitation hardening

Specimen designation	F_{max}, N	Overlap length A, mm	Joint width, mm	Joint surface area, mm^2	Shear strength R_t, MPa
G5/S/A	34450	4.02	25.51	102.6	336
G10/S/A	29898	4.06	25.47	103.4	289
G15/S/A	23799	3.96	25.41	100.6	237
G20/S/A	26282	4.19	25.58	107.2	245
G30/S/A	27443	4.07	25.43	103.5	265
G40/S/A	26900	4.05	25.53	103.4	260
G50/S/A	20284	3.97	25.42	100.9	201

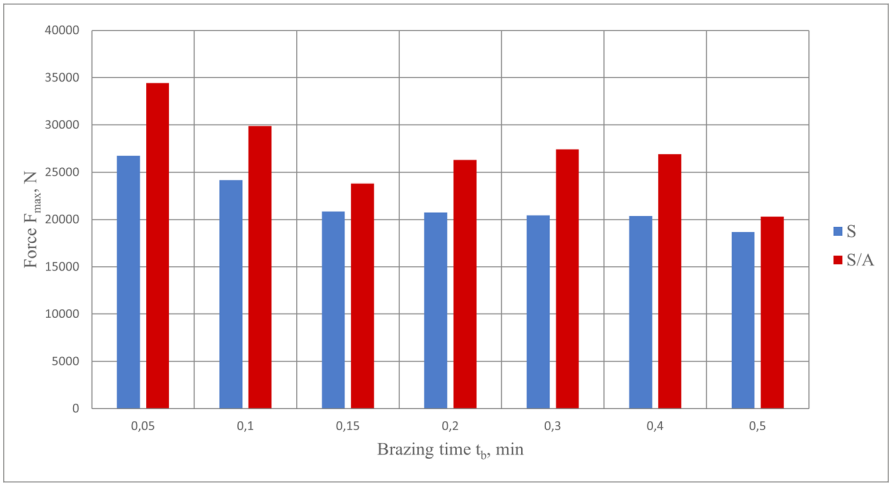

Fig. 13. Impact of the brazing gap on shear strength of the Inconel 718/Palnicro 36M joints after brazing with solutionizing and precipitation hardening

(Fig. 14b) to 70% for joint G50/S (Fig. 14c). Another noteworthy observation is the different location of the uncovered areas, which are found in the vicinity of the paste application area. It can be observed that these surfaces were wetted by the liquid BFM, but without forming a connection between them. Since the peel test aims to determine the percentage of the joint surface where a continuous connection has been established between the joined elements, these areas were classified as uncovered.

4. Discussion

The conducted research enabled the characterization of the influence of key parameters in the high temperature, vacuum furnace brazing process, namely braze time and gap width, on the properties of the Inconel 718/Palnicro 36M joints. Microstructure observation shows, that under conditions preventing isothermal crystallization in the entire volume of the joint, a complex, multiphase zone is formed – so called athermal solidification zone (ASZ). In case of materials adopted for test, this zone consist of two phase components: a dark-grey, plate-like precipitates of Ni-Pd-Cr phase, often also containing Fe addition (e. g. joints T1/S and T3/S) and Pd-Ni-Si-B phase, in form of continues, white bands located between Ni-Pd-Cr crystals. Another observable constituent is a very fine, dark precipitates of Cr-rich phases, concentrated mostly along the BM surface. Similar description of the microstructure morphology of the braze zone in the joints brazed using Palnicro 36M filler metal has been reported in the lit-

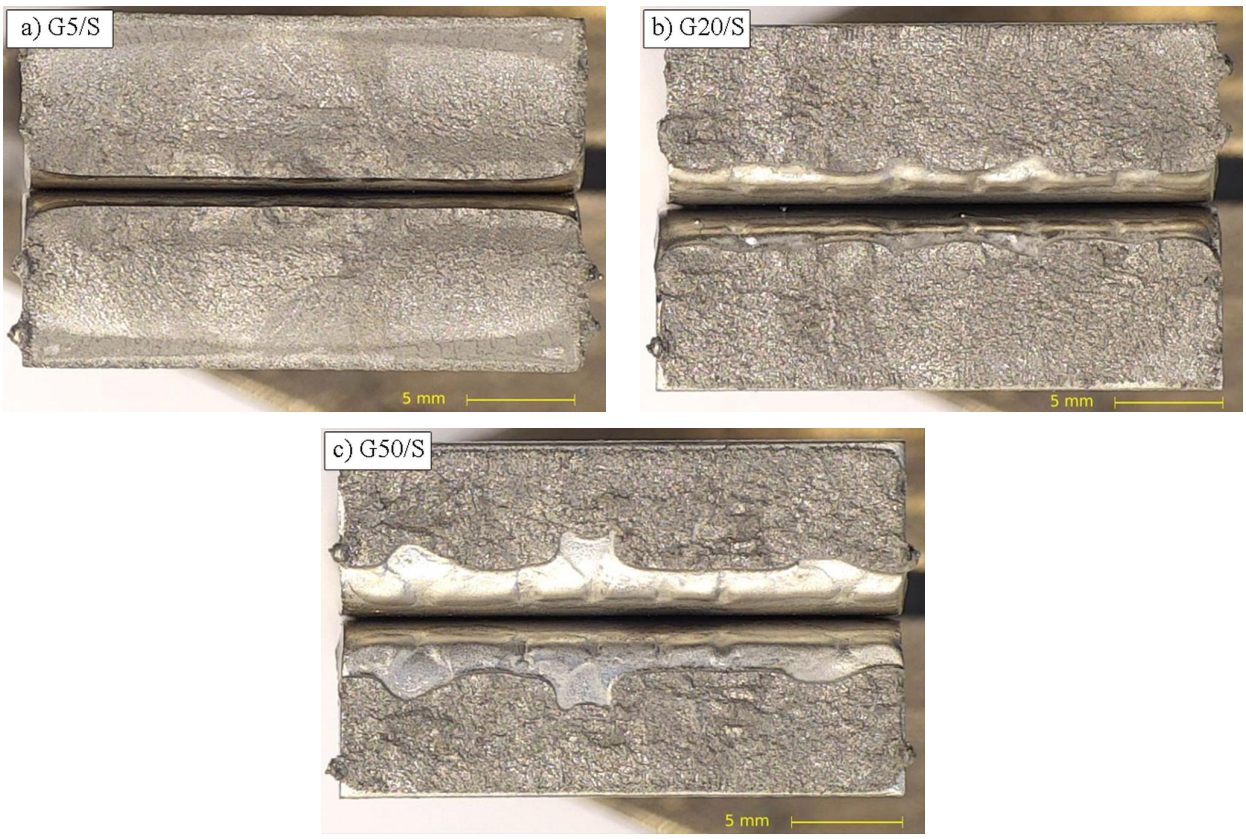

Fig. 14. View of brazed surfaces of Inconel 718/Palnicro 36M joints after peel test for gap width of 0.05 (a) and 0.3 mm (b)

erature [30]. The obtained results indicate the width of the brazing gap as the primary factor determining the evolution of the microstructure. It is particularly evident in the results of the first segment of the study, where presence of the ASZ was observed at the extremes of the analysed range of brazing time. The connecting factor for these joints was the width of the braze gap, exceeding the nominally assumed 50 μm. Results from that segment also show, that change of brazing time within 1-60 min range does not affect the coverage of joined surfaces and above 20 min of brazing time there is no further increase of BFM spreadability, which sets this time as a reasonable, technological limit that should be used in brazing processes. Moreover, change in brazing time within analysed range, does not have impact on depth or morphology of the diffusion zone of Inconel 718/Palnicro 36M joints. Finally, the conducted shear tests indicate a beneficial impact of extending the brazing time in the range of 1-10 min, beyond which no further influence on the joint mechanical properties was observed. Precipitation hardening operation resulted in general increase of the joints shear strength, while maintaining the trend associated with the brazing time or gap width observed prior to it. Ageing also clearly impacts the microstructure of the joints. Its main effect, observed in vast majority of the cases, is reduction of the Pd-rich phase relative volume in the ASZ. However, without more detailed investigation, it is not possible to formulate unequivocal conclusion regarding the influence of the final heat treatment on the microstructural changes. The second part of the study, aimed for investigation of gap width impact on the joint, confirmed its leading role in microstructure shaping. Obtaining uniform, single-phase microstructure of the braze zone was possible only for the smallest analysed gap of 0.05 mm (Fig. 12a, b). For each subsequent examined gap width, the presence of the ASZ was observed, and its relative volume increased with the widening of the gap. For values above 0.3 mm, this zone constitutes almost the entire volume of the braze. The peel test results indicate a gap width of 0.15 mm as the critical value, beyond which 100% coverage of the joined surfaces of Inconel 718 alloy sheets with Palnicro 36M filler metal is possible for the adopted lap length (8 mm). The increase in gap width also adversely affects the shear strength of the examined joints, as conclusively demonstrated by the analysis of the results obtained from the conducted strength tests. All these results combined can be used as a basis for identifying the optimal processing parameters in designing a brazing process cycle, both from a technological and economic perspective.

5. Conclusion and summary

In this study, the results of investigations of key parameters of the brazing process – brazing time and gap width – using Inconel 718 alloy as the BM and Palnicro 36M BFM are presented. Based on the conducted research, the following conclusions can be formulated:

- The dominant factor in shaping the microstructure of Inconel 718/Palnicro 36M joints is the width of the brazing gap.

- While maintaining a gap width not exceeding 0.05 mm, the brazing time sufficient for complete isothermal crystallization of the braze zone and obtaining a single-phase microstructure in it, is 10 min. Microstructure analysis, strength test and peel test results indicate it as the most optimal brazing time from both technological and economic perspectives.
- Under conditions insufficient for the occurrence of isothermal crystallization throughout the joint volume, the formation of an athermal crystallization zone, composed of a mixture of Ni-Pd-Cr and Pd-Ni-Si-B phases, occurs in the centerline of the joint.
- In the analyzed brazing time range – 1 to 60 min – and under the assumed conditions, each value within the range allows for achieving 100% coverage of the joined surfaces.
- In the brazing process concurrent with solutionizing, for a brazing time of 10 min, achieving a homogeneous joint microstructure is only possible for a 0.05 mm gap. Widening the gap results in the formation of ASZ, with its relative volume increasing with the gap width.
- Increasing the gap width above 0.15 mm leads to a decrease in the surface coverage and a deterioration in the mechanical properties of the joint.

Acknowledgments

Research carried out within the framework of the "Doktorat wdrożeniowy" (Implementation PhD) program – 2nd edition – funded by the Ministry of Education and Science.

REFERENCES

[1] A.D. Bartolomeis, S.T. Newman, I.S. Jawahir, D. Biermann, A. Shokrani, J. Mater. Process. Tech. **297**, 117260 (2021). DOI: https://doi.org/10.1016/j.jmatprotec.2021.117260.

[2] H. Eiselstein, D. Tillack, Superalloys 1-14 (1991). DOI: https://doi.org/10.7449/1991/SUPERALLOYS_1991_1_14

[3] S. Roy, R. Kumar, A. Kajla, A. Panda, Mater. Today-Proc. **5** (9), 18664-18673 (2018). DOI: https://doi.org/10.1016/j.matpr.2018.06.212

[4] S. Biswas, S. Ramachandra, P. Hans, S.P. Suresh Kumar, J. Indian. I. Sci. **102**, 297-309 (2022). DOI: https://doi.org/10.1007/s41745-022-00295-z

[5] D.F. Paulonis, J.J. Schirra, Superalloys 13-23 (2001). DOI: https://doi.org/10.7449/2001/Superalloys_2001_13_23

[6] M. Chaturvedi, Y.F. Han, Met. Sci. **17**, 145-149 (1983). DOI: https://doi.org/10.1179/030634583790421032

[7] C. Slama, M. Abdellaoui, J. Alloy. Compd. **306** (1-2), 277-284 (2000). DOI: https://doi.org/10.1016/S0925-8388(00)00789-1

[8] M. Jouiad, E. Marin, R.S. Devarapalli, J. Cormier, F. Ravaux, C. Le Gall, J.M. Franchet, Mater. Design. **102**, 284-296 (2016). DOI: https://doi.org/10.1016/j.matdes.2016.04.048

[9] https://www.specialmetals.com/documents/technical-bulletins/inconel/inconel-alloy-718.pdf, accessed: 15.12.2023.

[10] K. Krystek, K. Krzanowska, M. Wierzbińska, M. Motyka, Arch. Metall. Mater. **67** (4) 1551-1561 (2022). DOI: https://doi.org/10.24425/amm.2022.142375

[11] M. Way, J. Willingham, R. Goodall, R. Int. Mater. Rev. **65** (5), 1-29 (2020). DOI: https://doi.org/10.1080/09506608.2019.1613311

[12] Y. Sun, Z. Wang, Weld. World. **67**, 1299-1312 (2023). DOI: https://doi.org/10.1007/s40194-023-01470-1

[13] S. Azadian, L.Y. Wei, R. Warren, Mater. Charact. **53** (1), 7-16 (2004). DOI: https://doi.org/10.1016/j.matchar.2004.07.004

[14] S.H. Zhang, H.Y. Zhang, M. Cheng, Mat. Sci. Eng. **528** (19-20), 6253-6258 (2011). DOI: https://doi.org/10.1016/j.msea.2011.04.074

[15] I. Dul, J. Senkara, M. Bober, J. Jakubowski, Weld. Tech. Rev. 85 (9), 15-19 (2013).

[16] K. Linkiewicz, M. Baranowski, T. Babul, S. Kowalski, Arch. Metall. Mater. **60** (1), 159-165 (2015). DOI: https://doi.org/10.1515/amm-2015-0025

[17] M. Pouranvari, Mat. Sci. Tech. Ser. **31** (14), 1779-1780 (2015). DOI: https://doi.org/10.1179/1743284715Y.0000000005

[18] M. Pouranvari, A. Ekrami, A.H. Kokabi, Mat. Sci. Tech. Ser. **30** (1), 109-115 (2014). DOI: https://doi.org/10.1179/1743284713Y.0000000320

[19] G. Yan, A. Bhowmik, B. Nagarajan, X. Song, S. Chyn Tan, M. Jen Tan, Appl. Surf. Sci. 484, 1223-1233 (2019). DOI: https://doi.org/10.1016/j.apsusc.2019.04.070

[20] G. Yan, A. Bhowmik, B. Nagarajan, X. Song, S. Chyn Tan, M. Jen Tan, Mater. Sci. Eng. 766, 138267 (2019). DOI: https://doi.org/10.1016/j.msea.2019.138267

[21] S. Ghaderi, F. Karimzadeh, A. Ashrafi, J. Manuf. Process. **49**, 162-174 (2020). DOI: https://doi.org/10.1016/j.jmapro.2019.11.005

[22] Y. Zhishui, L. Ruifeng, S. Kun, Appl. Mech. Mater. **236-237**, 26-30 (2012). DOI: https://doi.org/10.4028/www.scientific.net/AMM.236-237.26

[23] M.A. Arafin, M. Medraj, D.P. Turner, P. Bocher, Mater. Sci. Eng. **447**, 125-133 (2007). DOI: https://doi.org/10.1016/j.msea.2006.10.045

[24] D. Bose, A. Datta, N. D. Cristofaro, Welding Research Supplement, 1983.

[25] M. Baranowski, J. Senkara, Weld. Tech. Rev. **91** (10), 51-58 (2019). DOI: https://doi.org/10.26628/wtr.v91i10.1078

[26] https://www.morganbrazealloys.com/media/dimbu50h/wesgo_palnicro-36m_technical-data-sheet-2018.pdf, accessed: 15.12.2023.

[27] American Welding Society (AWS) Committee on Brazing and Soldering: Brazing Handbook (5th ed.). American Welding Society, Miami FL 2007.

[28] A. Ghasemi, M. Pouranvari, Sci. Technol. Weld. Joi. **24** (4), 342-351 (2019). DOI: https://doi.org/ 10.1080/13621718.2018.1553280

[29] A. Ghasemi, M. Pouranvari, Sci. Technol. Weld. Joi. **23** (5), 441-448 (2018). DOI: https://doi.org/ 10.1080/13621718.2017.1410341

[30] M. Baranowski, J. Senkara, Materials **16** (3), 1115 (2023). DOI: https://doi.org/ 10.3390/ma16031115